Arab J Sci Eng (2014) 39:6411–6420
DOI 10.1007/s13369-014-1290-5

RESEARCH ARTICLE - MECHANICAL ENGINEERING

Strengthening of Bisphenol-A Epoxy Resin by the Addition of Multi-Wall Carbon Nanotubes

Muhammad Mansoor · Muhammad Shahid · Amir Habib

Received: 15 May 2013 / Accepted: 31 October 2013 / Published online: 8 July 2014

Abstract Multi-wall carbon nanotubes (MWCNTs) were prepared by chemical vapour deposition and purified by thermal oxidation. The purified MWCNTs were functionalized by nitric acid and hydrogen peroxide processes, and subsequently, the MWCNTs were added in bisphenol-A epoxy to prepare 0.1 % CNT- nanocomposites. Transmission electron microscopy, fourier transform infrared spectroscopy, rheological and mechanical testing showed that the MWCNTs functionalized by hydrogen peroxide processes were comprehensively de-roped causing their better dispersion and curing of the epoxy, which consequently resulted in higher mechanical properties of the nanocomposite. During fractography of the fractured specimens, a transition of the fracture behaviour was observed; smooth brittle fracture with fissure-like features having parallel planes perpendicular to crack propagation (in neat epoxy specimens) is transformed into mixed type fracture comprising variable angle steps like and fish scale like features (in functionalized CNT and epoxy specimens), which is indicative of the improvement in the fracture toughness.

Keywords Bisphenol-A · Carbon nanotubes · Chemical modification · TEM · FTIR · Rheology · Mechanical properties · Fractography

M. Mansoor · M. Shahid (✉) · A. Habib
School of Chemical and Materials Engineering, National University of Sciences and Technology, Islamabad, Pakistan
e-mail: shahidmet@yahoo.com; mshahid@scme.nust.edu.pk

الخلاصة

تم بوساطة ترسيب الأبخرة الكيميائي تحضير أنابيب الكربون النانوية متعددة الجدران ، وتنقيتها عن طريق الأكسدة الحرارية. وتمت إضافة مجموعات وظيفية إلى أنابيب الكربون النانوية متعددة الجدران المنقاة بوساطة عمليات حمض النيتريك وبيروكسيد الهيدروجين ، وفي وقت لاحق أضيفت أنابيب الكربون النانوية متعددة الجدران في ايبوكسي ثنائي الفينول-أ لإعداد تراكيب نانونية تحوي 0.1 ٪ من أنابيب الكربون النانوية. وأظهرت مجهرية انتقال الإلكترونات ، ومطيافية الأشعة تحت الحمراء المحولة بفوريه ، والاختبارات الريولوجية والميكانيكية أن أنابيب الكربون النانوية متعددة الجدران المفعلة من خلال عمليات بيروكسيد الهيدروجين كانت غير مشدودة بشكل شامل مسببة لأفضل تشتت وعلاج للايبوكسي، مما أدى بالتالي إلى خواص ميكانيكية أعلى للمركب النانوني. وقد لوحظ خلال رسومات كسر العينات وجود انتقال في سلوك الكسر؛ حيث يتم تحويل الكسر الهش على نحو سلس مع ميزات شق مثل وجود مستويات متوازية وعمودية لانتشار الكسر (في عينات الايبوكسي النقية) إلى كسر من نوع مختلط يتألف من ميزات مثل خطوات الزاوية المتغيرة وحجم الأسماك (في عينات أنابيب الكربون النانوية متعددة الجدران المفعلة والايبوكسي) الذي يدل على تحسن في صلابة الكسر.

1 Introduction

Bisphenol-A (BPA) is one of the most widely used thermosetting epoxy resin for industrial applications. These epoxies have higher mechanical properties, good chemical and corrosion resistance, high adhesion and dimensional stability with low shrinkage during curing [1]. Carbon nanotubes (CNTs) have extraordinary mechanical properties attributed by their exceptionally higher aspect ratios, which make them a promising reinforcing material for polymer nanocomposites [2–4]. CNT-based polymer nanocomposites have instigated a new era in material science by the transition of reinforcing material from micron to nanometer scale. Conversely, the possibility of pragmatic CNT reinforcement in polymers has been largely hampered by their poor dispersion and weak interfacial bonding with the polymer matrix [5–7]. The issue

could be alleviated by chemical modification of the CNTs, resulting in their better dispersion in the matrix [4,8]. Sheng-Hao et al. and Sharon et al. have reported similar approach to increase the dispersion of CNTs in the epoxy resin [9,10].

Previously, many researchers have reported a variety of chemical modifications (functionalization) of CNTs and their effects on different properties of CNT-polymer nanocomposites. Breton et al. [11] investigated the influence of micro-texture, structure and surface chemistry of multiwall carbon nanotubes (MWCNTs) on the improvement of the elastic modulus of nanotube-based composites. Fidelus et al. [12] reported that significant improvement (70 % reinforcement) in tensile impact strength was obtained for the 0.5 wt% MWCNTs/epoxy system. Progress in reinforcing epoxy matrix with fluorinated single-walled CNTs has also been reported [13]. The research of Song et al. [14] proves that dispersion states of CNTs in epoxy composites were extremely important.

The primary aim of this study was to explore the effect of dispersion states of MWCNTs on structural and mechanical of CNT-polymer nanocomposite, rendered by two chemical modification processes; (a) nitric acid and b) hydrogen peroxide based functionalization.

2 Experimental

2.1 Synthesis of MWCNTs

A chemical vapour deposition rector was used to synthesise MWCNTs by floating catalyst (FCCVD) technique. Cobalt acetate and ethanol were used as catalyst and carbonaceous source, respectively. The reactor temperature was 750 °C with a constant flow of argon to maintain reaction rate throughout the process. MWCNTs were collected on a copper substrate during the process. A schematic illustration of floating catalyst chemical vapour deposition (FCCVD) process is shown in Fig. 1. These MWCNTs were purified by thermal oxidation at 450 °C for 1 h to remove amorphous carbon. Further, the CNTs were treated with hydrochloric acid, in refluxing conditions, for 2 h to remove catalyst particles. To eliminate any functional groups, which might be produced during the purification processes, the CNTs were heated to 1,000 °C in nitrogen [15]. Subsequently, the MWCNTs were chemically modified by following two separate processes:

(a) Nitric acid process: The MWCNTs were treated with HNO_3, as described by Wang et al. [16]. Briefly, the CNTs were treated in a solution of HNO_3 and H_2SO_4(1:3 respective ratio) for 6 h at 50 °C under refluxing conditions. The process was followed by thorough rinsing with de-ionized water and filtration. The conductivity of the water was 10 µs. After filtration, the CNTs were treated at 65 °C for 45 min to eliminate residual moisture. These CNTs were named *"MWCNT-N"* for further reference.
(b) Hydrogen peroxide process: A 30 % solution of hydrogen peroxide and water was used to modify the CNTs. The process was carried out in a refluxing unit at 25 °C for 12 h. A subsequent washing and filtration was carried out as described earlier. These CNTs were named 'MWCNT-P.'

2.2 Composite Preparation

To prepare the composite, following procedure was carried out; required amount of pristine and modified MWCNTs (both N and P) were separately dissolved in 3:1 solution of ethanol and toluene. Typically, 100 mg MWCNTs were dissolved in 20 ml of the solution to prepare 0.1 % CNT-polymer composite. The mixture was sonicated for 20 min to disperse the nanotubes thoroughly without evaporating any of the solution. Later, the mixture was added to the required amount of the BPA. Magnetic stirring was carried out at 60 °C to disperse the nanotubes in BPA until ethanol, and toluene solution was completely evaporated, leaving a homogeneous mixture. Evaporation of the solvents was ensured by a 20 ml ca. volumetric solution loss. Subsequently, 64.5 g of the hardener (70-acid anhydride) and 1.94 g of the accelerator (dimethyl benzyl amine) were added for 100 g of BPA. The mixture was stirred until it became homogeneous, and then, it was then poured in tensile specimen moulds. To cure the composite, the moulds were heated at 80, 120, and 160 °C for 2 h at each temperature. Figure 8a shows the transmitted light image of the specimens after curing. A noticeable difference in transparency is present in various types of the specimens.

The nomenclature used in proceeding sections is given in Table 1.

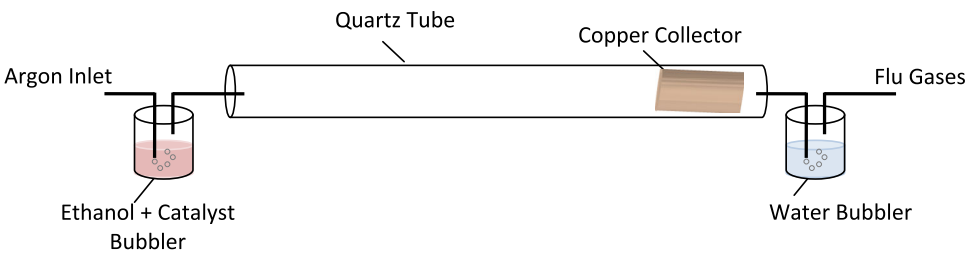

Fig. 1 Schematic diagram of the FCCVD reactor

Table 1 The nomenclature of the specimens

S. no.	Specimen chemistry	Specimen ID
1.	GY-2600 + Hardener + Accelerator. (neat epoxy)	Neat epoxy
2.	GY-2600 + Hardener + Accelerator + pristine MWCNTs	NC-O
3.	GY-2600 + Hardener + Accelerator + MWCNT-N	NC-N
4.	GY-2600 + Hardener + Accelerator + MWCNT-P	NC-P

2.3 Characterization

After chemical modifications, MWCNT-N and MWCNT-P nanotubes were characterized by using a transmission electron microscope (TEM) operating at 120KV. For specimen preparation, the CNTs were dispersed in ethanol by sonication and a droplet of the dispersion was dropped on a carbon coated TEM grid.

Fourier transformed infrared spectroscopy (FTIR) of the MWCNTs and the composite specimens was carried out at a resolution of 4 (cm^{-1}) in the range of 650–4,000 (cm^{-1}).

The rheological measurements were measured using a cone and plate geometry apparatus with the cone diameter of 40 mm and the cone angle of 2°. All the rheological measurements were carried out at 60 °C prior to the addition of hardener and accelerator.

Flexure and tensile tests were performed to evaluate mechanical characteristics of the neat epoxy and the nanocomposites using a 100 kN universal testing machine. A three-point bend test was carried out to measure the flexural strengths. Testing procedure was followed in accordance with ASTM D790-03 standard. For tensile testing (ASTM D638-03), a cross-head speed of 0.5 mm/min was used. All the tests were performed at room temperature. A set of five specimens was used from each type of testing.

Fractured surfaces of the tensile specimens were observed using SEM. A thin layer of gold coating was applied using sputtering technique to improve the imaging in the SEM.

3 Results and Discussion

3.1 TEM Analysis

Figure 2 represents TEM micrographs of MWCNT-N and MWCNT-P specimens. In micrograph (a), the CNTs are still in rope formation. Chemical modification process has only caused surface defects and uncapping of the tubes ends. CNTs are so tightly and bulkily roped that it was hard to reveal their transmission images. To reveal the roped condition of the MWCNTs, thermogravimetric analysis of the same specimens was also carried out in air, which showed (Fig. 2c) an increase in oxidation temperature of roped MWCNTs in comparison with un-roped MWCNTs, such an increases in oxidation temperature may indicate that the CNTs have either larger diameter or tangled rope formation [17]. In micrograph b), the CNTs are un-roped and individual CNTs could be seen in transmission mode. These CNTs are multi-walled with nominal diameter of 10nm. In isolated regions, segments of CNT ropes are also evident. A histogram of the diameter distribution of the CNTs is shown in Fig. 3. TEM studies depict towards the fact that in present study, modification with nitric acid curtailed the CNT un-roping, whereas hydrogen peroxide process un-roped the CNTs comprehensively.

3.2 FTIR Spectrum

FTIR spectra of MWCNTs before and after chemical modifications are shown in Fig. 4. In the functional group region (4,000–1,300 cm^{-1}) of the spectra, the peaks which are identified at 1,352, 1,785 and 3,259 cm^{-1} characterize C–O, C=O and O–H bonds in the nanotubes, respectively. Peaks at 1,785, 1,647 and 3,259 cm^{-1} can be attributed to carboxyl group as well [18,19]. Peak at 1,647 cm^{-1} assigns C=C bond in CNTs which is appeared after disappearing of bond symmetry because of connection of oxygenated functional groups [20,21]. In low-frequency region (909–650 cm^{-1}), presence of the peak 837 cm^{-1} indicates aromatic C–H bending of CNT carbon atoms. The fingerprint peak-F represents O–H out of plane bend at 1,037 cm^{-1} [21].

As the addition of CNTs in epoxy has no significant effects on absorption band in uncured condition [21], FTIR studies were focused on cured specimens only. Figure 5 shows the FTIR spectra of the BPA, NC-O, NC-N and NC-P after curing. Presence of epoxide groups is associated with transmittance bands in the region 800–920 cm^{-1} [22,23] and [24]. Usually, changes in the transmittance band are attributed to the curing of the epoxy [24]. The transmittance intensity of this band is considered maximum for un-cured epoxy resins, which accordingly decreases with the conversion of the epoxide groups during the curing cycle [24,25].

In FTIR spectra (Fig. 5), the shift of reference band intensities occurred in nanocomposites specimens when compared with neat epoxy. A maximum shift of the band occurred in case of pristine MWCNTs (i.e. NC-O), while it lowered in case of functionalized MWCNTs (i.e. NC-N and NC-P). A minimum shift was observed in NC-P specimens. The shift of intensities bands depicts towards the fact that presence

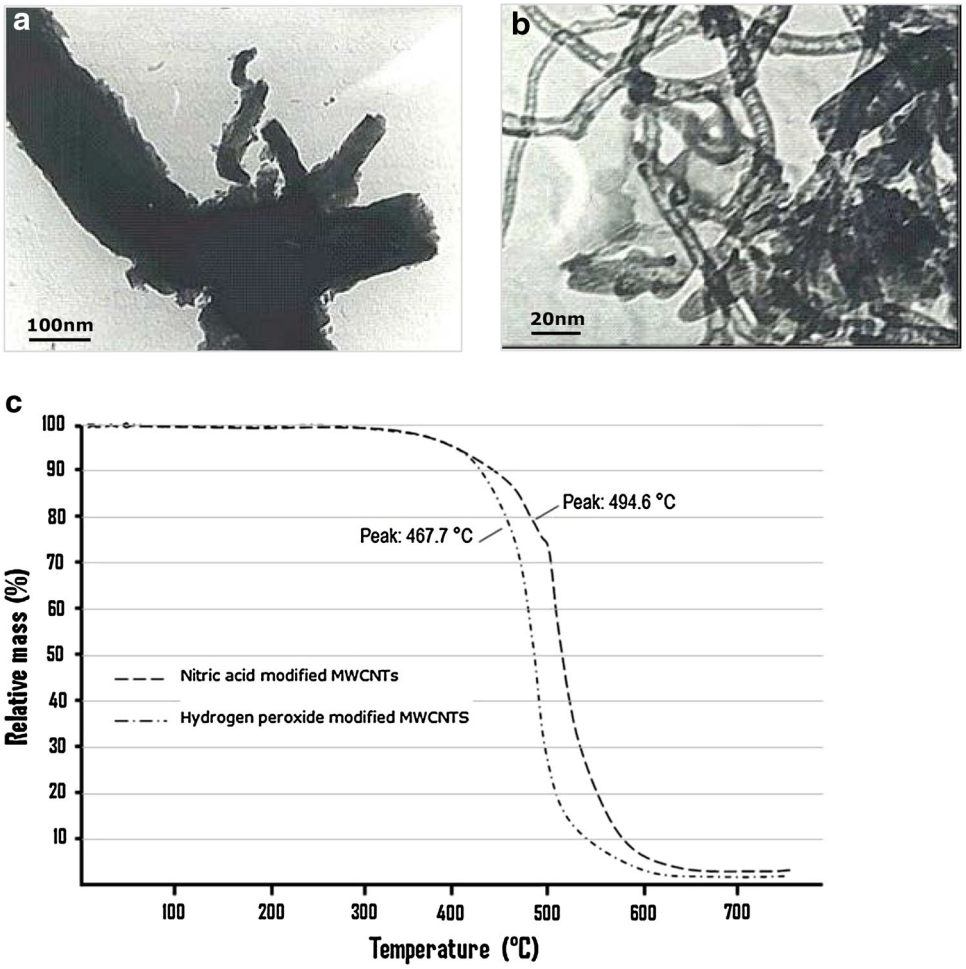

Fig. 2 **a** and **b** TEM micrographs of MWCNTs modified by nitric acid and hydrogen peroxide processes, respectively. **c** TGA curves of nitric acid and hydrogen peroxide modified MWCNTs showing that roped MWCNTs **a** have higher oxidation temperature

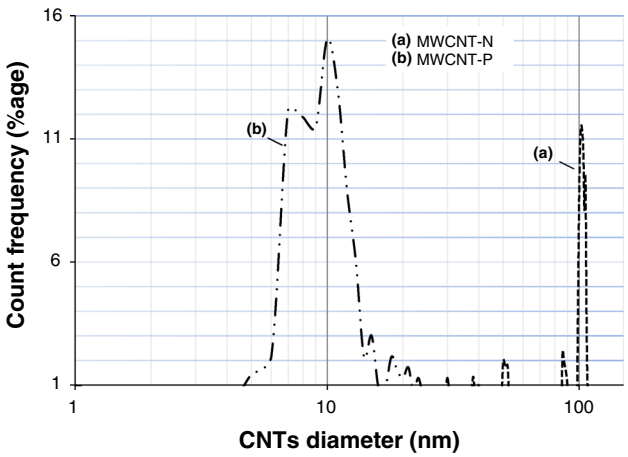

Fig. 3 Histograms of percentage diameter distribution of MWCNTs after chemical modification by *a* nitric acid and *b* hydrogen peroxide processes (*horizontal axis* is represented on log scale)

of MWCNTs influenced the extension of conversion bands of the epoxide groups. The extension of the bands was lowered as the added MWCNTs were more dispersed and unaccumulated or de-roped. The observation illustrates that incorporation of accumulated MWCNTs resulted insufficient curing during the experimental curing cycles. Such incomplete curing may result in subsequent lowering of global properties of the nanocomposites.

3.3 Viscosities

Figure 6 presents the viscosities of neat BPA, BPA + pristine MWCNT, BPA + MWCNT-N and BPA + MWCNT-P, solutions at 60 °C, as a function of shear rate. An increase of 2, 6 and 19 % in viscosities of BPA + pristine MWCNT, BPA + MWCNT-N and BPA + MWCNT-P solutions, respectively, in comparison with the neat resin was observed. The increase in viscosities could be attributed to extend the dispersion and/or exfoliation of CNTs in the matrix [26]. Moreover, Licea-Jimenez et al. [27] found that the increase in viscosities could be due to the suppression in the formation of vortices in the presence of CNTs. Albeit, specimen MWCNT-N was functionalized yet the CNTs were in bundles and were not fully available to disperse in the matrix. Contrarily, specimen MWCNT-P was un-roped and fully available for dispersion (Fig. 2). The un-roping of CNTs after functionalization could

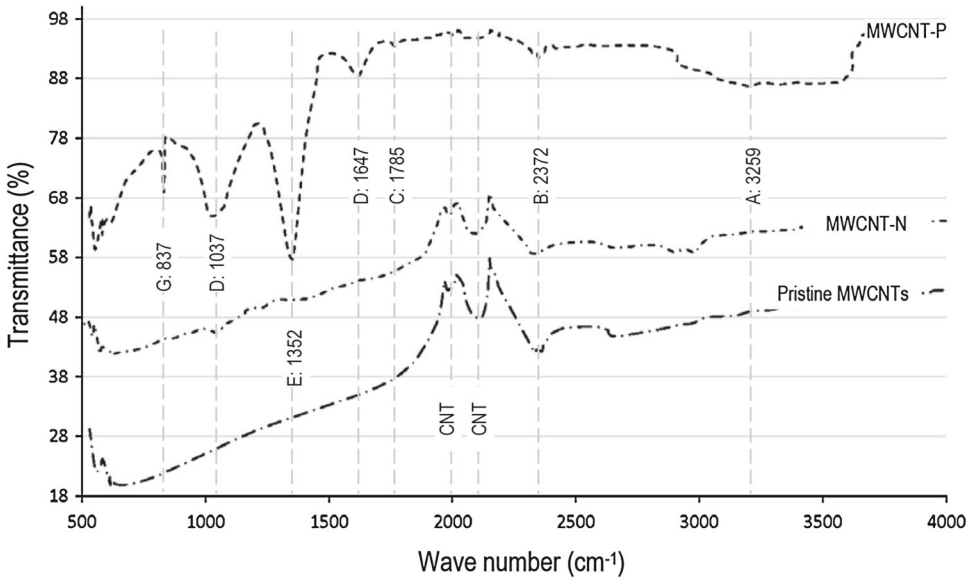

Fig. 4 FTIR spectra of MWCNTs before and after chemical modifications

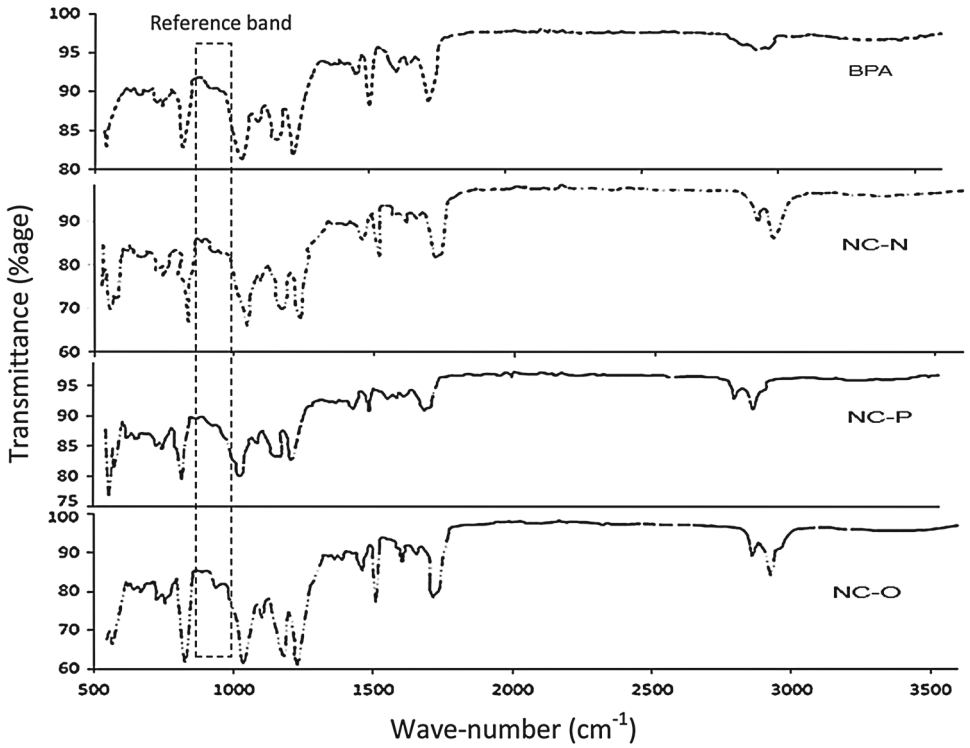

Fig. 5 FTIR spectra of various cured specimens of the neat epoxy and nanocomposites

be a potential factor to disperse CNTs in the matrix, and consequently, an increase in viscosities was observed.

3.4 Mechanical Testing

During mechanical testing, flexure strengths of various nanocomposites were compared with the neat epoxy specimens. It was observed that in nanocomposites NC-O and NC-N, flexure strengths were decreased up to 10 % than that of neat epoxy, whereas a discernable raise of 41 % was found in NO-P specimens (Fig. 7). A similar comportment of the composites was also observed during tensile testing. In NC-O and NC-N specimens, a decrease of 2 % and increase of 23 % in tensile strength were occurred, respectively. In contrast, NC-P exhibited an augmentation of 135 % in ultimate tensile strength (Fig. 8). Moreover, NC-P specimens were more elastic (3.2 % elongation) as compare to the rest. In Fig. 8, it is also evident qualitatively that NC-P specimens have superior resilience and toughness than neat epoxy, NC-O and NC-N specimens. Similar types of results are quoted

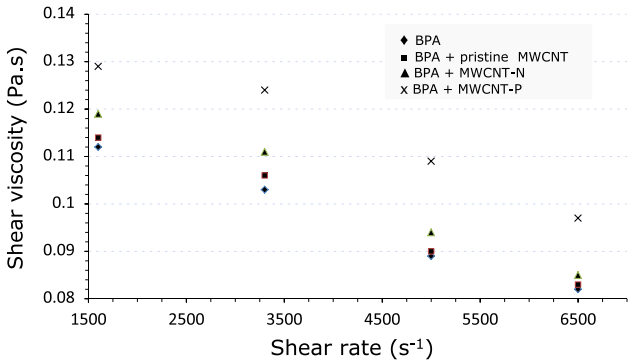

Fig. 6 Rheological behaviour of various un-cured epoxy specimens

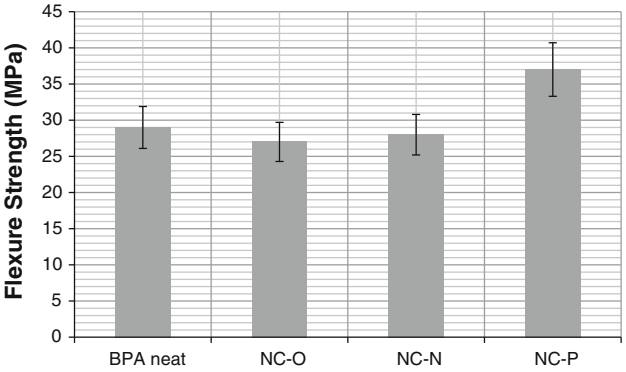

Fig. 7 Flexure strengths of various nanocomposites and neat epoxy

by Allaoui et al. [28], where they have studied the mechanical and electrical properties of the composite with different weight percentages of nanotubes.

The decrease in mechanical properties of nanocomposites NC-O and NC-N cloud be attributed by two main interlinked factors: first, the lowering of tensile strength due to the accumulation of CNTs as ropes/bundles; and second, the change in epoxy curing realm due to the accumulated MWCNTs. In Fig. 5, the effect of MWCNTs on the structure of cured epoxy nanocomposites is evident in respective FTIR spectra. In the case of NC-O and NC-N, the addition of accumulated MWCNTs caused a partial curing of the epoxy, whereas a relatively better curing was observed in NC-P specimens, where the MWCNTs were more de-roped (see Fig. 2). Partial curing of the nanocomposites (NC-O and NC-N) could be a rational account for their lower mechanical responses.

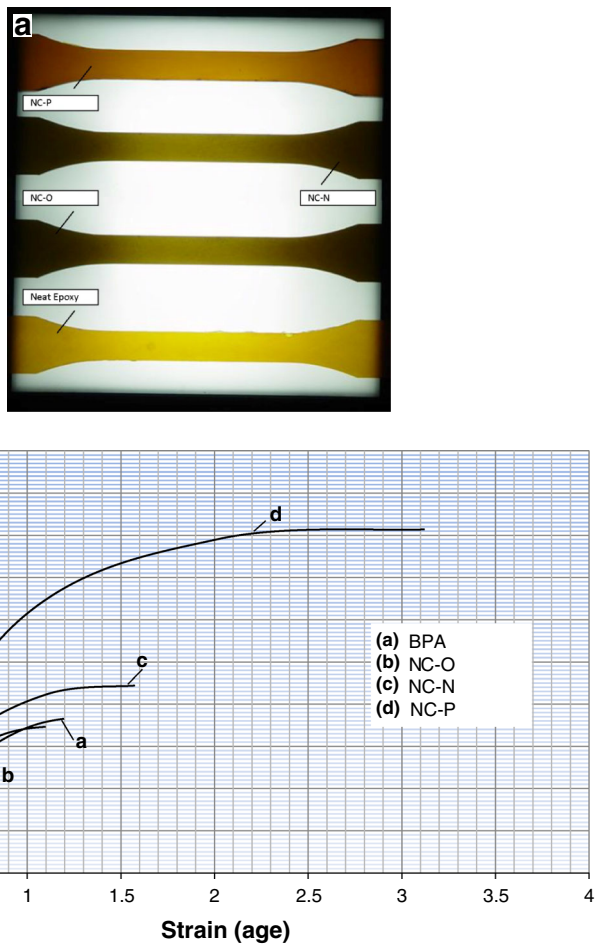

Fig. 8 **a** Transmitted light images of tensile specimens, **b** superimposed stress–strain curves of neat epoxy and various nanocomposites

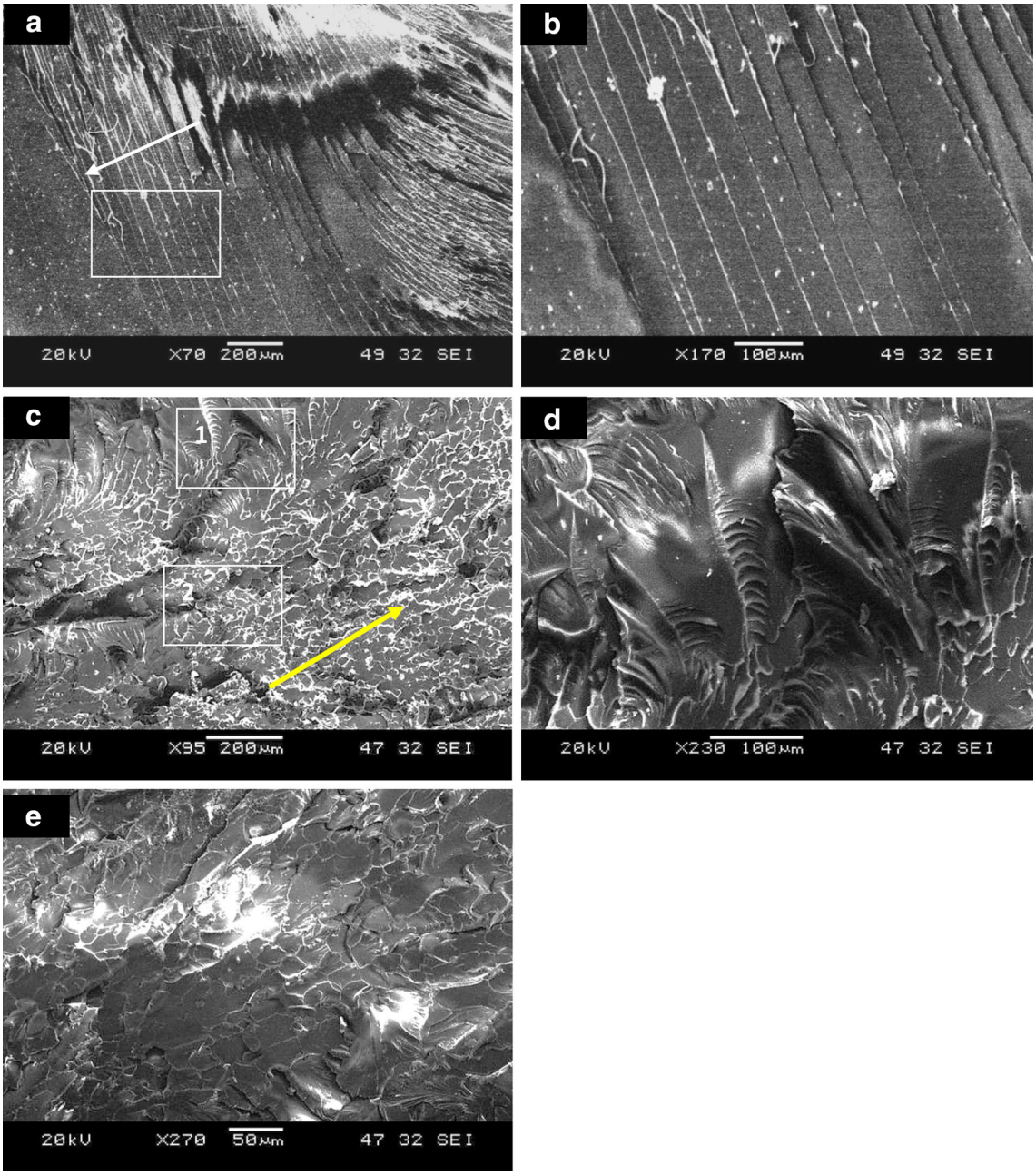

Fig. 9 Fracture surface of **a** 'BPA' revealing brittle fracture with fissures, **b** *boxed region* in **a** at high magnification revealing featureless surface between the fissures, **c** 'NC-O' revealing fissures as well as fish skin like mixed features, **d** and **e** high magnification of region '1' and '2', respectively; note the cracking in fracture surface (the *arrow* in figures indicates the crack propagation direction)

3.5 Fractography

Fracture surface of the BPA tensile specimens revealed smooth brittle fracture with fissure-like features having parallel planes perpendicular to crack propagation (Fig. 9a, b). The cleavage planes between the steps of fissures were featureless (Fig. 9b). It is indicative of the brittle failure having low toughness [29]. In the specimen 'NC-O','the fracture morphology was changed and a mixed type fracture was observed comprising of (i) variable angle steps like and (ii) fish scale like features as shown in Fig. 9c–e. Secondary cracking was also observed on the fracture surface (Fig. 9e).

In the fracture surface of NC-N nanocomposite, a flat featureless surface was observed next to the origin (Fig. 10a). In the latter stages of the fracture, hackle lines with fish scale like features were observed as shown in Fig. 10b. Hackle regions are associated with a more violent stage of fracture in which a large amount of strain energy is absorbed through

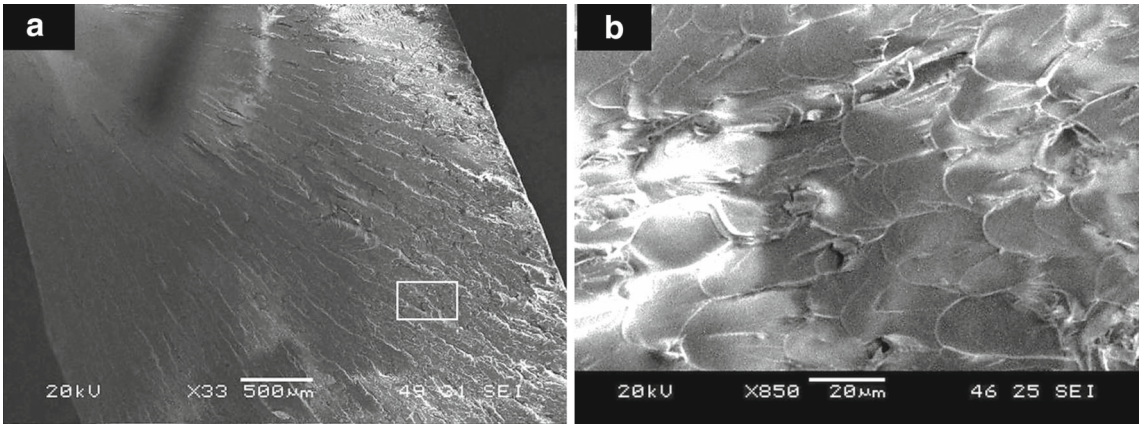

Fig. 10 Fracture surface of **a** NC-N nanocomposite, revealing featureless at crack initiation region and fish skin like regular pattern in the later stages of fracture, **b** the high magnification of the *boxed region* in **a** revealing fish skin like pattern

both plastic deformation and the generation of new fracture surface areas. These regions tend to appear in areas where the stress field is changing rapidly (either in direction or magnitude) or when the stress state changes from one of the plane strain to plane stress. Fish scale like features are probably due to the branching of the crack. For a material incapable of plastic deformation, such as glass or a polymer at a very low temperature with totally inoperative flow processes, crack branching is the only mechanism for increasing the rate of energy dissipation [30].

In the fracture surface of NC-P nanocomposite, the crack was initiated from smaller fissures which are indicative of the tensile stress dominance [31] as revealed in Fig. 11a. The next to the origin region was more tortuous compared with the fracture of NC-N due to CNTs distribution in the matrix. The increase in the roughness implies that the crack tip was distorted due to the CNTs presence; it makes crack propagation more difficult. The hackle region and the crack branching were observed in the later stages of the crack (Fig. 11c, d).

Fracture surface of the neat epoxy matrix reveals a brittle behaviour characterized by large smooth areas. These are characteristic of Mode-I loading and indicate a weak resistance to crack propagation. In contrast to the neat epoxy, nanocomposite (NO-P) surfaces typically show a micro-rough structure characterized by flow patterns aligned in the direction of the main crack propagation, along with hackle-like features. Such matrix shear deformation (shear yielding) may occur by an energy-consuming mechanism in a particulate filled epoxy resin, and the mechanism has been reported by several other energy-consuming mechanisms are expected to be particle de-bonding [32], crack front pinning and the initiation of secondary cracks at local inhomogeneities indicated by hyperbolic markings [29], such as observed as fish scale like features in CNT loaded epoxies.

SEM images of the fracture surfaces showed a more tortuous path of crack propagation around areas of high CNTs concentration in the nanocomposites (NC-P). The creation of additional surface areas on crack propagation was thus assumed to be the primary factor for the toughening effect (see Fig. 8) [33]. Similar findings were reported for nanocomposites based upon unsaturated polyester [34] or high functionality epoxy resin nanocomposites [35].

4 Conclusions

Multi-wall carbon nanotubes were synthesized by FCCVD, where ethanol was used as carbonaceous source and cobalt acetate was used as catalyst. MWCNTs were synthesized at 750 °C and deposited on a copper sheet. After thermal purification at 450 °C, the MWCNTs were functionalized by nitric acid and hydrogen peroxide process, i.e. MWCNT-N and MWCNT-P, respectively. These two types of MWCNTs and pristine MWCNTs were added in BPA epoxy and cured.

A comprehensive un-roping of the CNTs was attained by hydrogen peroxide process. A maximum percentage distribution for 10 nm diameter CNTs was realized. FTIR studies showed that both of the processes (i.e. nitric acid and hydrogen peroxide) successfully attached hydroxyl functional group to the MWCNTs. However, a better level of dispersion of CNTs was attained for MWCNT-P as discussed in viscosity measurements section.

After curing, the FTIR of NC-O, NC-N and NC-P specimens showed a lowering in extension bands with respect to the BPA specimens, which in turn is an indicative of an incomplete curing of the epoxy. The observation could be used to further extend the curing cycle for a complete epoxy curing, and subsequently, better global properties of the nanocomposites could be achieved. Maximum increase

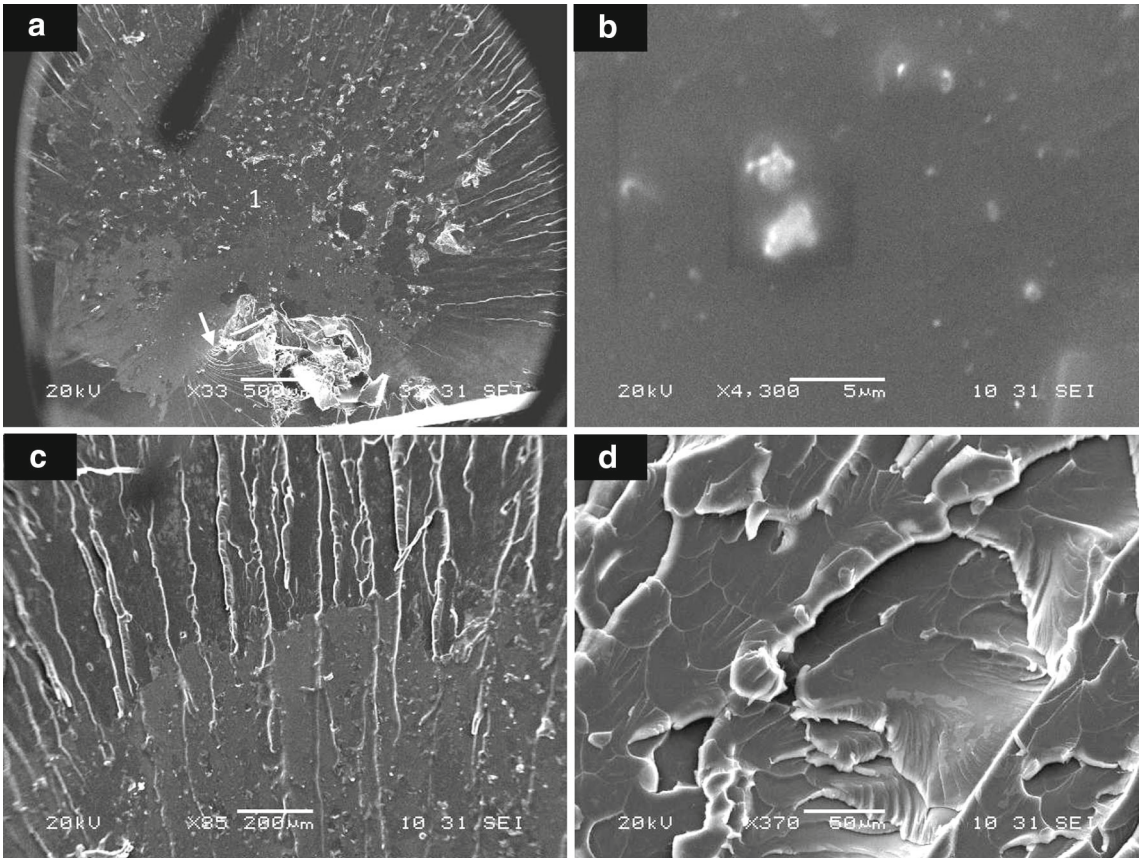

Fig. 11 Fracture surfaces of NC-P nanocomposite revealing **a** crack initiation from a fissure (*arrow*); **b** comparatively featureless region next to the origin showing embedded particulates, **c** heckle lines diverging away from the origin, **d** fish skin like regular pattern in the later stages of fracture

in flexure and tensile strengths was observed in NC-P specimens. This increase in mechanical properties was attributed to the inclusive dispersion of MWCNTs and better curing of the epoxy. In case of NC-O and NC-N, viscosity measurements and FTIR analyses showed a lower level of MWCNT dispersion and incomplete curing of the epoxy, respectively, which consequently caused reduction in the mechanical behaviour.

During fractography, it was found that the incorporation of well- dispersed and functionalized MWCNTs has changed the fracture behaviour of the composite. Presence of the MWCNTs caused an increase in the fracture surface roughness. The crack tip was subsequently distorted due to the MWCNTs presence which reduced the crack propagation. Moreover, it also caused an increase in the hackle region and the crack branching which is indicative of more energy absorption during fracture.

References

1. Joel, R.F.: Polymer Science and Technology. Pearson education ltd, Singapore (2006)
2. Unger, E.; Graham, A.; Kreupl, F.; Liebau, M.; Hoenlein, W.: Electrochemical functionalization of multi-walled carbon nanotubes for solvation and purification. Curr. Appl. Phys. **2**, 107–111 (2002)
3. Sun, X.K.; Zhao, W.M.: Prediction of stiffness and strength of single-walled carbon nanotubes by molecular-mechanics based finite element approach. Mater. Sci. Eng. A **390**, 366–371 (2005)
4. Jin, A.K.; Dong, G.S.; Tae, J.K.; Jae, R.Y.: Effects of surface modification on rheological and mechanical properties of CNT/epoxy composites. Carbon **44**, 1898–1905 (2006)
5. Chen, Q.; Dai, L.; Gao, M.; Huang, S.; Mau, A.: Plasma activation of carbon nanotubes for chemical modification. J. Phys. Chem. B **105**, 618–622 (2001)
6. Smrutisikha, B.: Influence of dispersion states of carbon nanotubes on mechanical and electrical properties of epoxy nanocomposites. J. Sci. Ind. Res. **66**(9), 752–756 (2007)
7. Nadia, G.; Joachim, L.; Lucas, L.; Maryse, M.; Ce'cile, Z.; Cor, E.; John, H.: High-conductivity polymer nano-composites obtained by tailoring the characteristics of carbon nanotube fillers. Adv. Funct. Mater. **18**, 3226–3234 (2008)
8. Sun, Y.P.; Fu, K.; Lin, Y.; Huqng, W.: Functionalized carbon nanotubes: properties and applications. Acc. Chem. Res. **35**, 1096–1104 (2002)
9. Sheng-Hao, H.; Ming-Chung, W.; Sharon, C.; Chih-Min, C.; Shih-Hsiang, L.; Wei-Fang, S.: Synthesis, morphology and physical properties of multi-walled carbon nanotube/biphenyl liquid crystalline epoxy composites. Carbon **50**, 896–905 (2012)
10. Sharon, C.; Sheng-Hao, H.; Ming-Chung, W.; Wei Fang, S.: Kinetics studies on the accelerated curing of liquid crystalline epoxy

resin/multiwalled carbon nanotube nanocomposites. J. Polym. Sci. B **49**, 301–309 (2011)
11. Breton, Y.; De'sarmot, G.; Salvetat, J.P.; Delpeux, S.; Sinturel, C.; Be'guin, F.: Mechanical properties of multiwall carbon nanotubes/epoxy composites: influence of network morphology. Carbon **42**, 1027–1030 (2004)
12. Fidelus, J.D.; Wiesel, E.; Gojny, F.H.; Schulte, K.; Wagner, H.D.: Thermo-mechanical properties of randomly oriented carbon/epoxy composites. Compos. A **336**, 1555–1561 (2005)
13. Miyagawa, H.; Rich, M.J.; Drzal, L.T.: Thermo-physical properties of epoxy composites reinforced by carbon nanotubes and vapor grown carbon fibers. Thermochim. Acta. **442**, 67–73 (2006)
14. Song, Y.S.; Youn, J.R.: Influence of dispersion states of carbon nanotubes on physical properties of epoxy composites. Carbon **43**, 1378–1385 (2005)
15. Naseh, M.V.; Khodadadi, A.A.; Mortazavi, Y.; Alizadeh, O.S.; Pourfayaz, F.; Sedghi, S.M.: Functionalization of carbon nanotubes using nitric acid oxidation and BDB plasma. Proc. World Acad. Sci. Eng. Technol. **37**, 177–179 (2009)
16. Yao, W.; Jun, W.; Fei, W.: A treatment method to give separated multi-walled carbon nanotubes with high purity, high crystallization and a large aspect ratio. Carbon **41**, 2939–2948 (2003)
17. Kim, D.Y.; Yang, C.M.; Park, Y.S.; Kim, K.K.; Jeong, S.Y.; Han, J.H.: Characterization of thin multi-walled carbon nanotubes synthesized by catalytic chemical vapor deposition. Chem. Phys. Lett. **413**, 135–141 (2005)
18. John, H.L.; Mauricio, T.; Elisabeth, M.; Katherine, E.H.; Vincent, M.: Evaluating the characteristics of multiwall carbon nanotubes. Carbon **49**, 2581–2602 (2011)
19. Robert, M.S.; Clayton, G.B.; Terence, C.M.: Spectrometric Identification of Organic Compounds, pp. 104–122. Wiley, New York (1981)
20. Zhao, C.; Ji, L.; Liu, H.; Hu, G.; Zhang, S.; Yang, M.; Yang, Z.: Functionalized carbon nanotubes containing isocyanate groups. J. Solid State Chem. **177**, 4394–4398 (2004)
21. Chingombe, P.; Saha, B.; Wakeman, R.J.: Surface modification and characterization of a coal-based activated carbon. Carbon **43**, 3132–3143 (2005)
22. Lau, K.T.; Lu, M.; Lam, C.K.; Cheung, H.Y.; Sheng, F.L.; Li, H.L.: Thermal and mechanical properties of single-walled carbon nanotube bundle-reinforced epoxy nanocomposites: the role of solvent for nanotube dispersion. Compos. Sci. Technol. **65**(5), 719–725 (2005)
23. Evtushenko, Y.; Ivanov, V.M.; Zaitsev, B.E.: Determination of epoxide and hydroxyl groups in epoxide resins by IR spectrometry. J. Anal. Chem. **58**(4), 347–350 (2003)
24. Hong, S.G.; Wu, C.S.: DSC and FTIR analysis of the curing behaviours of epoxy/DICY/solvent open systems. Thermochim. Acta **316**(2), 167–175 (1998)
25. Loos, M.R.; Coelho, L.A.F.; Pezzin, S.H.; Amico, S.C.: The effect of acetone addition on the properties of epoxy. Polím. Ciênc. Tecnol. **18**(1), 76–80 (2008)
26. Cotiuga, I.; Picchioni, F.; Agarwal, U.S.; Wouter, D.; Loos, J.; Lemstra, P.J.: Block-coploymer-assisted solubilization of carbon nanotubes and exfoliation monitoring through viscosity. Macromol. Rapid Commun. **27**(13), 1073–1078 (2006)
27. Licea-Jimenez, L.; Henrio, P.Y.; Lund, A.; Laurie, T.M.; Perez-Garcia, A.S.; Nyborg, L.: MWNT reinforced melamine-formaldehyde containing alpha-cellulose. Compos. Sci. Technol. **67**(5), 844–854 (2007)
28. Allaoui, A.; Bai, S.; Cheng, H.M.; Bai, J.B.: Mechanical and electrical properties of aMWNT/epoxy composite. Compos. Sci. Technol. **62**(15), 1993–1998 (2002)
29. Zhou, Y.X.; Wu, P.X.; Cheng, Z.; Jeelani, S.: Improvement in mechanical properties of epoxy by filling carbon nanotubes. Express Polym. Lett. **2**(1), 40–48 (2008)
30. ASM Metals Handbook, vol. 11—Failure analysis and prevention, ASM International Materials Park, Russell Township, Geauga County, pp. 2250–2260 (2002)
31. ASM Metals Handbook, vol. 11—Failure analysis and prevention, ASM International Materials Park, Russell Township, Geauga County, pp. 1387–1389 (2002)
32. Klaus, F.; Stoyko, F.; Zhong, Z.: Polymer composites from nano- to macro-scale. Polym. Compos. **5**, 51–54 (2005)
33. Becker, O.; Simon, G.P.: Epoxy layered silicate nanocomposites in: inorganic polymeric nanocomposites and membrane. Adv. Polym. Sci. **179**, 135–142 (2005)
34. Kornmann, X.; Berglund, L.A.: Nanocomposites based on montmorillonite and unsaturated polyester. J. Polym. Eng. Sci. **38**, 1351–1358 (1998)
35. Becker, O.: High performance epoxy-layered silicate nanocomposites. PhD in School of Physics and Materials Engineering. Monash University, Melbourne (2003)